SYNERGY BETWEEN SUSPENDING AGENT AND AIR ENTRANING AGENT IN CEMENT SLURRY

TAO LI[1,2] * , XIAOLONG WANG[1],MING LI[1], DEYI NAN[1],QIYUAN SHAN[2] , WEIXIN CHEN[2]

[1]*School of Energy and Mining Engineering, China University of Mining and Technology(Beijing), Beijing 100083, China;.*

[2]*College of Mining Engineering, Heilongjiang University of Science and Technology, Harbin 150027, China*

In cut-and-fill mining, cement slurry is piped over a long distance from the mixing plant to the filling site underground. The long-distance transport poses a challenge to the long-term rheological stability of cement slurry. If the properties are undesirable, the pipeline will be easily plugged, bringing the mining to a standstill. This paper carries out rheological experiments on four groups of cement slurries, which differ in the dosages of suspending agent (SA) and air entraining agent (AEA). The synergy between SA and AEA was verified through analysis on images captured by a scanning electron microscope (SEM) and an X-ray diffractometer (XRD). The results show that the optimal SA and AEA dosages are 0.045% and 0.009% respectively; under the synergy between SA and AEA, the rheological properties of cement slurry could be modified to achieve long-term rheological stability. The research results contribute to the long-term homogeneity and flowability of cement slurry, and improve the effects of cut-and-fill mining.

Keywords: *Long-Distance Pipeline Transport; Rheological Properties; Suspending Agent (SA); Air Entraining Agent (AEA); Synergy*

1. Introduction

Coal gangue-fly ash cement slurry is prepared by mixing coal gangue, fly ash, cement, and water at proper ratios. Cement slurry plays an important role in cut-and-fill mining. In general, cement slurry is piped from the preparation site to the mining area under pumping pressure and self-weight. As coalmine tunnels get deeper and longer, the length of the pipeline to transport cement slurry has being growing. It takes a long time for cement slurry to travel and repose through the long-distance pipeline. During the transport, the slurry components may go through complex physical and chemical processes, complicating the slurry motion. Both the filling efficiency and piping safety depend on the long-term rheological stability of cement slurry.

Many researchers have tried to improve the rheological properties of cement slurry in the piping stage of cut-and-fit mining. For instance, Yang et al. [1] tested the performance of a new cement slurry with different mix ratios, and learned that cement slurry achieved the best flowability in the pipeline, when the mix ratio is cement: lime: desulphurized gypsum: fly ash =10:1.8:9:79.2. Ye et al. [2] studied the law of motion state and resistance of large particles in the complex process of pipeline transport, and drew the following conclusions: the particle motions have three possible states in pipeline transport, namely, rolling, migration, and suspension; the resistance loss is positively correlated with mean velocity, volume concentration and density, but negatively with particle diameter and inner diameter of pipeline. Deng et al. [3] numerically simulated the pressure, flow rate and deflection features of cement slurries of different concentrations in pipeline, revealing that the concentration of 72-74% leads to good rheological properties and reduces the friction loss of the slurry in pipeline. Xu et al. [4] explored how particle diameter of coal gangue affects the rheological features of cement slurry in Xinyang Coalmine, and noticed the multiple, complex flow patterns in the entire flow process. Yang et al. [5] modelled the suspension mechanics of spherical and non-spherical coal gangue particles in transport, and concluded that adding fly ash and suspending agent (SA) can keep coal gangue particles in slurry suspended, improving the rheological properties of cement slurry. Deb et al. [6] discovered that the rheological properties, filling effect, and flowability of cement slurry depend directly on the physical properties, chemical composition, and mechanical properties of aggregates. Anubhav et al. [7] found that the pressure head loss of tailings-fly ash cement slurry should be calculated based on Bingham pattern, and that adding fine-grained particles like fly ash helps improve the homogeneity of cement slurry. Lee et al. [8] examined the effects of slurry concentration, fly ash content, temperature, and stirring time on the rheological properties of cement slurries with different flow patterns, pointing out that suitable fly ash content, stirring time, temperature and $CaCl_2$ content could improve the rheological properties and reduce the

* Autor corespondent/*Corresponding author*,
E-mail: Little6511945@126.com

friction loss of cement slurry.

The above studies shed important light on how to improve the rheological properties and flowability of cement slurry, and reduce the friction loss during pipeline transport [9, 10]. However, none of them have tackled the rheological properties of cement slurry in long-distance piping, during which the slurry moves and reposes for a long time.

This paper targets a coalmine in northern China's Hebei province. The coalmine has small remaining reserves of coal resources, part of which lies beneath residential areas. This part of coal resources needs to be mined to increase the recovery rate. However, the traditional roof collapse treatment may cause the surface to collapse, posing a threat to the nearby buildings and residents. Therefore, the cut-and-fill mining was adopted to mine the coal resources beneath the residential areas [11, 12]. During the mining, a 3,800m-long pipeline was installed between the mixing plant to the filling site underground. It takes at least 115min for cement slurry to travel and repose in the pipeline, calling for the long-term rheological stability of the slurry. Hence, it is a must to ensure the suspending state and good flowability of cement slurry in the long term. As a result, this paper carries out rheological experiments on coal gangue-fly ash cement slurry, and analyzes the experimental results in details.

2. Experimental Background

The rheological properties of cement slurry are affected by various factors, including concentration of slurry, content and type of cementitious material, content of fly ash, shape and physical-chemical properties of aggregates, particle diameter of aggregates, as well as mixing temperature and method [13]. Through repeated experiments, the optimal concentration of cement slurry for the target coalmine was determined as 70.2%, and the optimal mix ratio as cement: fly ash: coal gangue: water =12:19.5:38.7:29.8.

As mentioned before, it takes about 35min for cement slurry to move through the 3,800m-long pipeline. The mean flow rate is 1.8m/s. As the subsections of the coalface are filled in sequence, cement slurry needs to repose for about 80min in the pipeline. If no filling failure occurs, the total time of cement slurry in the pipeline amounts to 115min. Over such a long time, the flow state of the slurry is complicated by the complex chemical reactions between its components. The dosages of slurry components must be adjusted to optimize the rheological properties of the slurry. Here, SA and air entraining agent (AEA) are added into the slurry, aiming to keep the slurry homogenous in suspending state with a small loss of flowability.

Comparative experiments show that, without adding AEA, the best suspending effect was achieved at the SA dosage of 0.035%. However, under this SA dosage, cement slurry was partially condensed, inducing a large loss of flowability. In this case, the long-distance pipeline would be plugged, making it extremely inefficient to transport cement slurry to the filling site. To protect long-term flowability, the AEA was also added to cement slurry. Hence, this paper attempts to identify the optimal dosages and disclose the synergy mechanism of AEA and SA. Under the constant temperature of 25℃, comparative experiments were performed on four groups of the two agents in different dosages. The compositions of cement slurries in each group are listed in Table 1, where DF is a kind of starch ether; ST is a saponin non-ionic surfactant.

3. Materials, Apparatuses and Process

The cement slurries were prepared from water, cement, fly ash and coal gangue. The chemical compositions of fly ash and coal gangue were measured by an Ultima X-ray diffractometer

Table 1

Compositions of cement slurries in each group

No.	Cement content (%)	Fly ash content (%)	Coal Gangue conent (%)	Water content (%)	Slurry concentration (%)	SA DF (%)	AEA ST (%)
1	12	19.5	38.7	29.8	70.2	0.035	0
2	12	19.5	38.7	29.8	70.2	0.035	0.004
3	12	19.5	38.7	29.8	70.2	0.035	0.009
4	12	19.5	38.7	29.8	70.2	0.045	0.009

Table 2

Semi-quantitative analysis results of the energy spectrum of coal gangue

Chemical components	Al_2O_3	SiO_2	S	K_2O	CaO	TiO_2	Fe_2O_3
Mass percent (%)	23.64	42.65	3.8	0.73	22.73	1.17	5.28

Table 3

Semi-quantitative analysis results of the energy spectrum of fly ash

Chemical components	Al_2O_3	SiO_2	S	K_2O	CaO	TiO_2	Fe_2O_3
Mass percent (%)	32.79	55.98	0.77	1.28	1.75	1.97	5.46

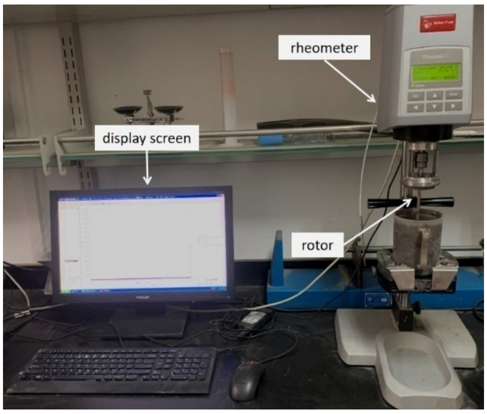

(a) RheolabQC rheometer

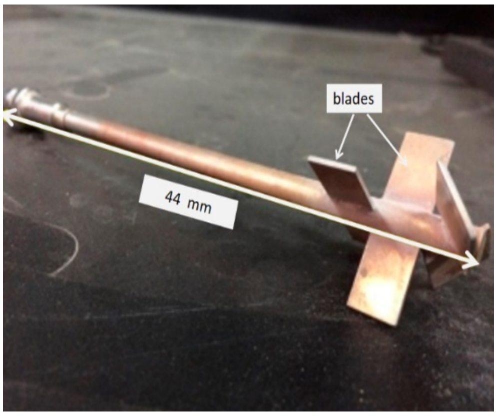

(b) Rotor

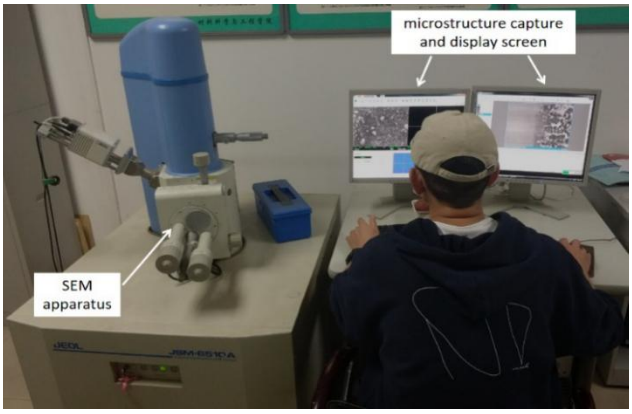

(c) SEM

Fig. 1 - Experimental apparatuses.

(XRD). The measured results are recorded in Tables 2 and 3. It can be seen that the fly ash and coal gangue are mainly composed of SiO_2 and Al_2O_3.

As mentioned before, the optimal concentration of cement slurry for the target coalmine was determined as 70.2%, and the optimal mix ratio as cement: fly ash: coal gangue: water =12:19.5:38.7:29.8.

A RheolabQC rheometer (Figures 1a and 1b) was adopted for our experiments to measure the shear stress and viscosity at different agent dosages and shear rates. Before the measurement, the rotor was placed in a 500mL beaker filled with cement slurry. During the measurement, the shear rate, preloaded to 50 1/s for 10s, was increased from 50 to 160 1/s for 120s.

Four groups of cement slurries were tested every 30min from 0min to 120min. Besides, the slurry in each group was cured for 28d into hardened blocks. After that, the structure and morphology (Figure 1c) of their hydrates were scanned by a JEOL JSM-6510A scanning electron microscope (SEM).

4. Experiments on Rheological Properties of Cement Slurry

4.1 Rheological parameters

Viscosity and yield stress are two basic rheological parameters of cement slurry as a non-Newtonian fluid. Viscosity is a measure of internal friction resistance, which is an inherent physical property of non-Newtonian fluids in the presence of relative motion. For cement slurry, the relative motion refers to the deformation under external shear force, which results in the internal friction resistance to the deformation. Reflecting the friction angle and cohesion of the cement slurry, viscosity is the macroscale property of the microscale actions among slurry molecules. The level of viscosity depends on multiple factors, namely, cement content, particle diameter distribution, slurry concentration, and the momentum exchange among solid and liquid molecules.

Yield stress refers to the minimum shear stress of the slurry flow. Despite some arguments about its existence, yield stress is a default property of cement slurry in the rheological theory on slurry flow. This property directly bears on the slump and flowability of cement slurry [14, 15].

4.2 Rheological patterns

By flow rate, the varied flow states of cement along the pipeline can be divided into laminar flow state and turbulent flow state. Once the slurry concentration reaches a threshold, cement slurry will become excessively viscous, leading to great changes to slurry features [16, 17]. Based on rheological properties, cement slurry could be a

Table 4

Typical rheological patterns

Rheological patterns	Constitutive equations
Newtonian pattern	$\tau=\eta\gamma$
Bingham pattern	$\tau=\tau_0+\eta\gamma$
Herschel-Bulkley pattern	$\tau=\tau_0+\eta\gamma^n$
Power equation pattern	$\tau=A\gamma^n$
Ostwald-dewaecle pattern	$\tau=\tau_0+B\sin^{-1}(\gamma/C)$
Eyring pattern	$\tau=a\gamma^n+B\sin^{-1}(\gamma/C)$
Robertson-Stiff pattern	$\tau=a(\gamma+C)^b$
Atzeni et al.'s pattern	$\tau=a\tau^2+\beta\tau+\delta$

Note: A, a, B, b, C, K, α, β, and δ are constants; τ is shear stress; τ_0 is yield stress; η is viscosity; γ is shear rate.

Newtonian fluid or non-Newtonian fluid. Table 4 sums up the possible rheological patterns of cement slurry.

Previous studies have shown that high-concentration cement slurry has a much smaller Reynolds number than a fluid in the transition from laminar to turbulent flow. The most suitable rheological pattern for high-concentration cement slurry is Herschel-Bulkley pattern [4,18]. Under this pattern, the constitutive equation can be expressed as:

$$\tau = \tau_0 + \eta\gamma^n \tag{1}$$

where, τ is shear stress, Pa; γ is shear rate,1/s; η is viscosity, Pa·s; τ_0 is yield stress, Pa; n is flow index. When n=1 and τ_0=0, the rheological pattern is Newtonian pattern; When n=1 and τ_0>0, the rheological pattern is Bingham pattern; When n>1, the rheological pattern is expansion pattern; When n<1, the rheological pattern is pseudo plastic pattern.

4.3 Fitting and analysis of rheological parameters

The rheological data on the four groups of cement slurries were measured at 0, 30, 60, 90 and 120min, and fitted by formula (1) into the rheological curves in Figure 2. The rheological parameters of each group at each time point were derived from the curves and recorded in Table 5. It can be seen that, with the elapse of reposing time, the four groups witnessed a growth in hydration reaction and the completion of a mesh structure, pushing up the viscosity and yield stress of cement slurry [19, 20].

As shown in Figure 3, the four groups varied in terms of rheological parameters in the same period. Group 1 had the highest viscosity, followed in turn by Group 2, Group 4, and Group 3. This is because Group 1 has zero AEA, while Groups 3 and 4 have the highest AEA dosages. The AEA introduces lots of microbubbles into cement slurry. Their lubrication effect makes the slurry less consistent and viscous. Moreover, Groups 2-4 had much lower viscosity and yield stress than Group 1; the higher the AEA dosage, the smaller the values of the two parameters.

In the same period, Group 4 was more viscous than Group 3, for the former had a higher SA dosage and a more complete mesh structure. The two factors work together to reduce the slurry flowability, and increase viscosity and yield stress to some extent.

In addition, the viscosity of Group 1 increased to 2.71 times at 120min, the largest increment among all four groups. This means the cement slurry in this group is partially condensed, with a high loss of flowability. At 120min, the viscosity values of Groups 3 and 4 increased to 1.96 and 1.86 times, respectively. The viscosity growth of these two groups was slow, indicating that the corresponding cement slurries maintained the best flowability.

The reason for the phenomenon above is that the directional adsorption of AEA microbubbles negatively charges the hydration micro-clusters on the surface of cement or cement particles. The negative charge disperses the particles by electrostatic repulsion, preventing cement particles from forming a mesh structure (Figure 6). The growing spacing between particles slows down the further condensation of the floc structure and the hydration process inside the slurry. As a result, Groups 3 and 4 suffered the smallest viscosity loss, and maintained a good flowability.

As shown in Table 5, the flow index n of Group 1 remained as 1 during 0-90min. In this period, the cement slurry in Group 1 maintains a stable flow state and belongs to non-Newtonian and Bingham pattern. At 120min, the flow index n values of Groups 2 and 3 were smaller than 1, a sign of flow pattern variations [21]. In this case, these two slurries belong to the pseudoplastic pattern, that is, the long-term rheological stability is poor, and the coarse aggregates in the slurries have partially sedimented. The flow index n of Group 4 was equal to 1 throughout the experiment. This means the cement slurry in Group 4 belongs to Bingham pattern and maintains good homogeneity and long-term rheological stability. The slurries with long-term rheological stability are suitable for long-distance piping. However, the cement slurry in Group 1 lost much of its viscosity and partially condensed, which affect its suitability for long-distance piping.

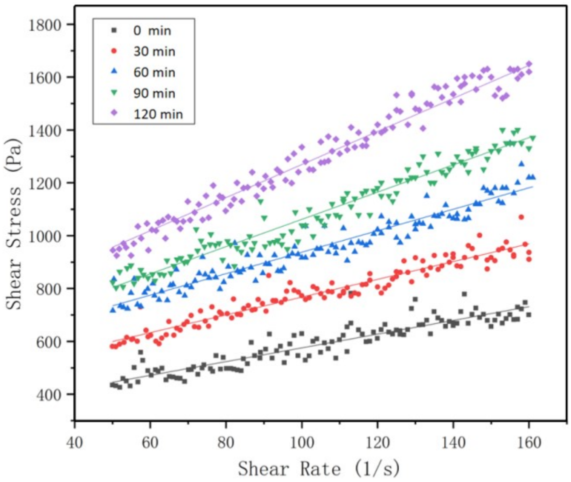

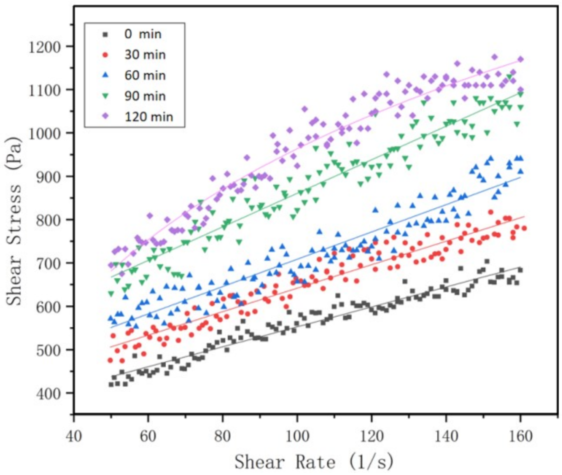

(a) Group 1 (b) Group 2

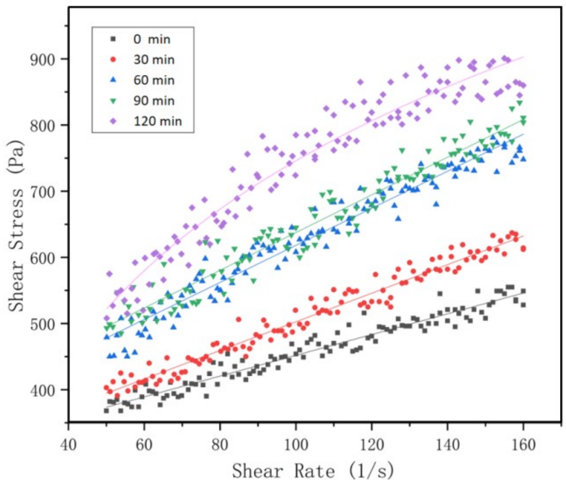

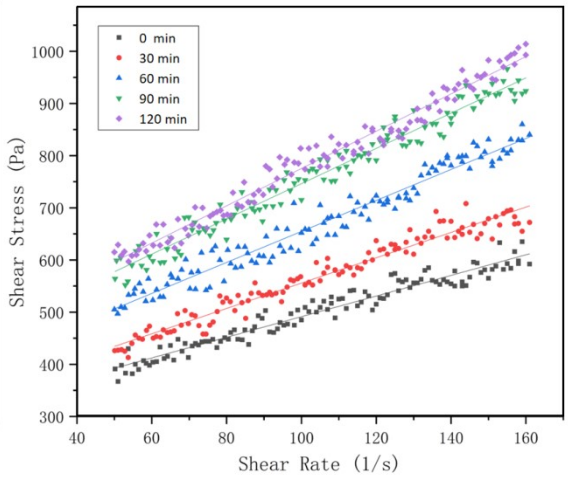

(c) Group 3 (d) Group 4

Fig. 2 - Rheological curves.

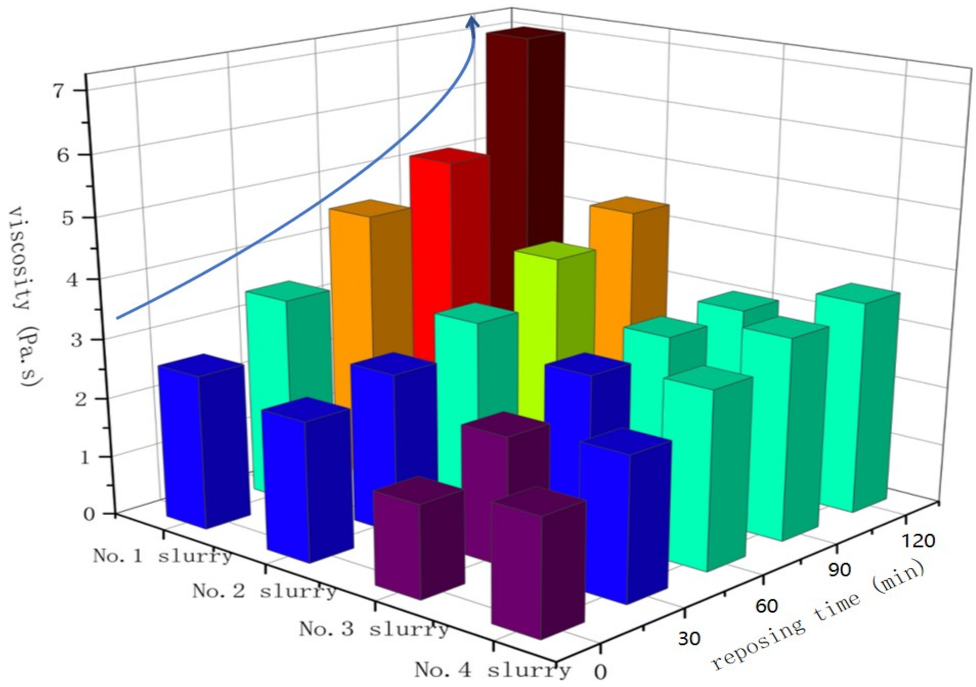

Fig.3 – Viscosities of four groups at different time points.

Table 5

Rheological parameters of four groups at different time points

Reposing time/min	Rheological index	Group 1	Group 2	Group 3	Group 4
0	η (Pa·s)	2.5989	2.3433	1.5491	1.9304
	τ_0 (Pa)	434	419	368	391
	n	1	1	1	1
	R^2	0.8469	0.9321	0.9363	0.9262
30	η (Pa·s)	3.4719	2.6833	2.1618	2.3981
	τ_0 (Pa)	581	475	403	426
	n	1	1	1	1
	R^2	0.9361	0.8807	0.9662	0.9398
60	η (Pa·s)	4.545	3.1497	2.7336	2.9792
	τ_0 (Pa)	716	571	479	505
	n	1	1	1	1
	R^2	0.907	0.8639	0.9286	0.8968
90	η (Pa·s)	5.1579	3.8698	2.9681	3.3989
	τ_0 (Pa)	823	630	493	564
	n	1	1	1	1
	R^2	0.9326	0.9264	0.9258	0.9206
120	η (Pa·s)	7.0395	4.3353	3.0400	3.5895
	τ_0 (Pa)	945	695	508	615
	n	1	0.4544	0.4646	1
	R^2	0.9696	0.9548	0.9324	0.9591

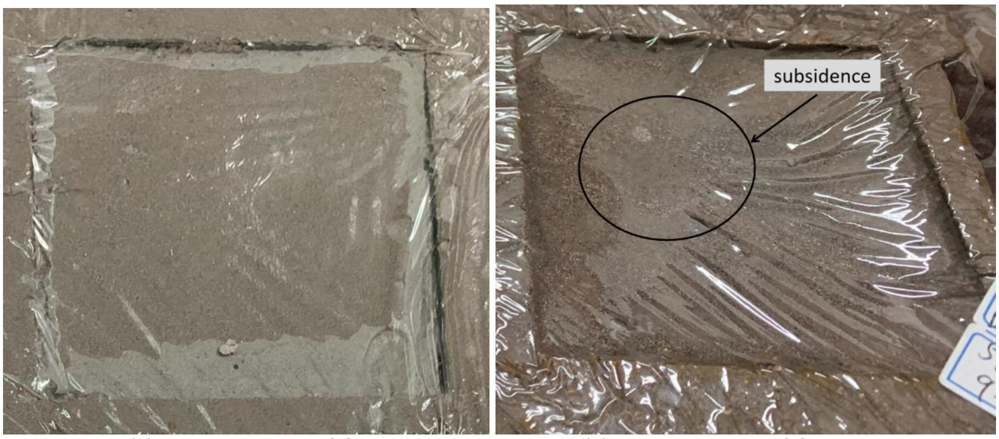

(a) Hardened block of Group 1 (b) Hardened block of Group 2

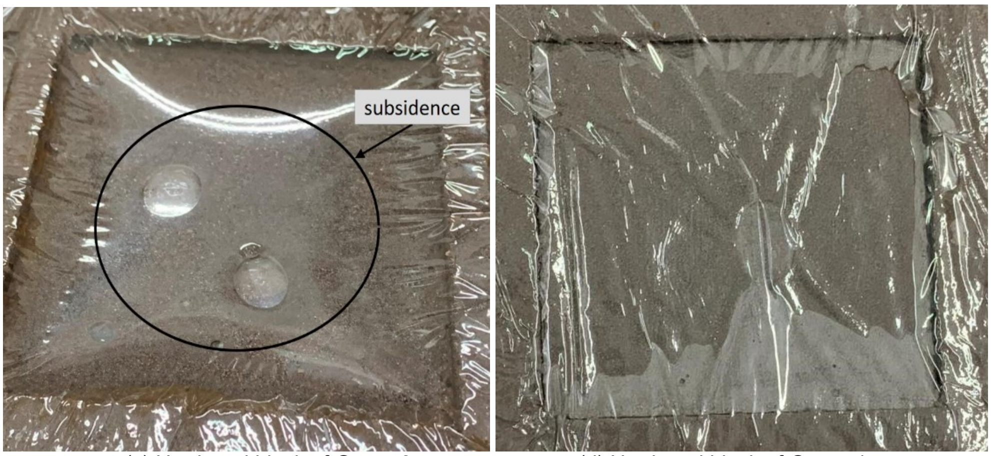

(c) Hardened block of Group 3 (d) Hardened block of Group 4

Fig. 4–8h appearances of hardened blocks in the four groups.

During the experiments, Group 3 went through serious condensation. The corresponding hardened block showed an obvious subsidence on the upper surface (Figure 4c). After 8h, the block could not stand out from the mold, making mining and filling inefficient. Group 3 and 4 have the same AEA dosage, and only differs in SA dosage. As shown in Figure 4d, there was no condensation in Group 4, and the hardened block could stand out from the mold after 8h.

The internal condensation and upper surface subsidence of hardened block of Group 3 should be further studied at different SA dosages, in view of the synergy between SA and AEA in the same slurry. The physical and chemical synergy between the two agents determines the long-term rheological stability of cement slurry, as well as the suitability of cement slurry for long-distance piping.

5 Synergy between SA and AEA

5.1 Action mechanism of SA and AEA

(1) Action mechanism of SA DF [22]

Once dissolved in cement slurry, the SA will be evenly dispersed in the cement slurry system. As shown in Figure 5, the DF molecular chains form a mesh structure, which will adsorb fine particles like cement and its initial hydration clumps, fly ash, and fine aggregates. These molecular chains bridge up fine particles into a mesh of suspending chains, making cement slurry more viscous and resistant to stress. The mesh, distributed like a yarn inside the cement slurry, prevents or slows down the gravity-induced sinking of coarse aggregates, and achieves the effect of suspending homogenization.

(2) Action mechanism of AEA ST [23]

The AEA ST is an anionic surfactant. The ST molecules produces and stabilizes micro-bubbles by changing the following properties of cement slurry: surface tension, particle surface charge, surface viscosity and gas permeability. Under the action of the AEA, hundreds of millions of micro-bubbles are produced per cubic meter, which are not connected and evenly distributed. These micro-bubbles lubricate the transport of cement slurry, and fill in the voids of slurry particles. In this way, the micro-bubbles could reduce the loss of internal energy caused by particle friction during transport, making the slurry much less consistent and viscous.

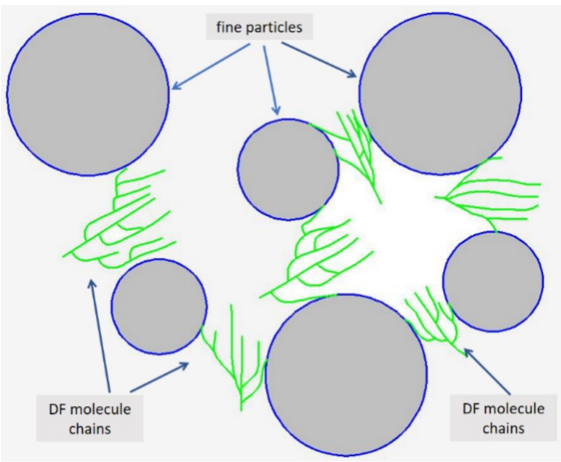

Fig. 5 - DF molecules

The micro-bubbles are adsorbed by the hydration clumps of cement and cement particles, causing the particles to be negatively charged. The particles with the same charge repel and disperse each other. This electrostatic repulsion curbs the formation of the intergranular floc structure in Figure 6. The growing distance between cement particles limits the further condensation of the floc structure, enabling the cement slurry to better maintain its flowability.

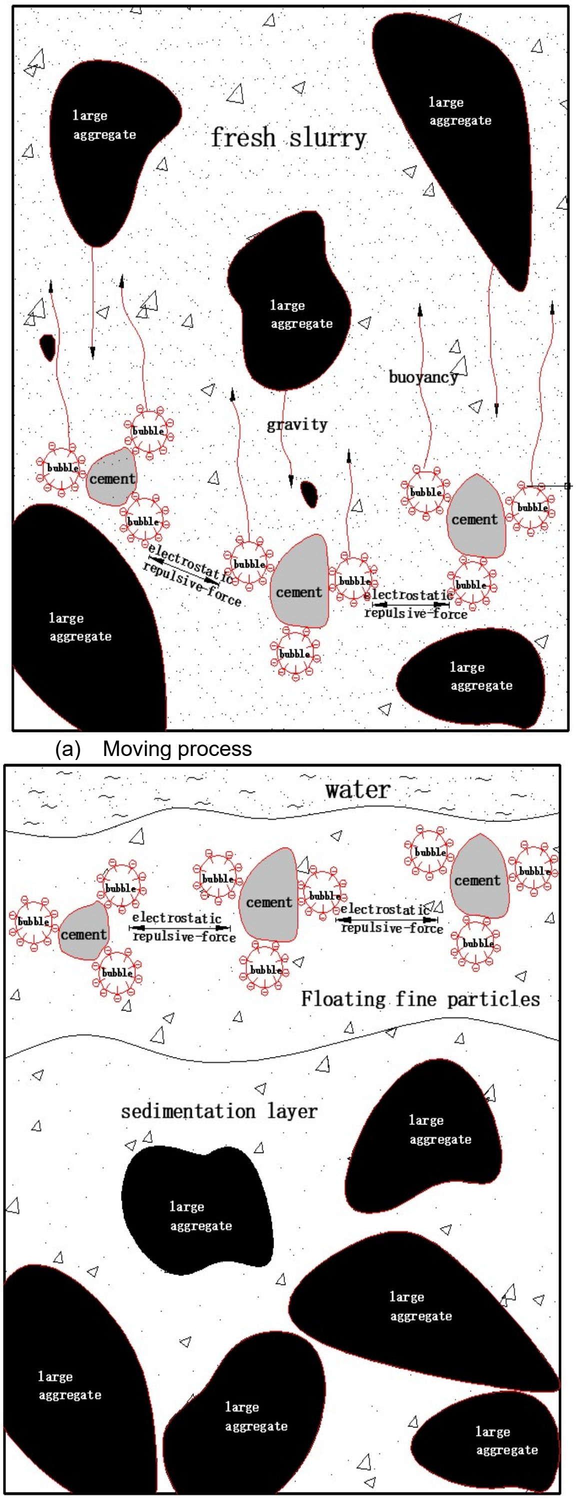

(a) Moving process

(b) Delamination

Fig. 6 - Delamination of cement slurr

5.2 Synergy mechanism

The synergy between SA and AEA refers to the coordination and cooperation between the two additives to achieve the same goal. The synergistic effect is generally stronger than the individual effects combined. The SA DF molecular chains form a mesh structure, which contains the micro-bubbles created as AEA adsorbs fine particles. In return, the micro-bubbles lubricate the structure, and support and expand the structure, due to their floating and separation effects. Under the combined effects of SA and AEA, the cement slurry is not delaminated but homogeneous. The synergy between SA and AEA magnifies the effects of the two additives.

The SA DF molecular chains adsorb fine particles, producing a mesh structure inside the cement slurry. The system supports the coarse aggregates in the slurry, keeping the slurry homogenous and stable. The integrity and coverage of the system depend on the dosages of DF, cement, fly ash, and fine aggregates. Enough DF molecular chains guarantees the completeness of the mesh structure inside the slurry, keeping coarse aggregates suspending. If the amount of DF molecular chains is insufficient, there will not be a complete mesh structure, not to mention the suspension of coarse aggregates.

The micro-bubbles produced by the AEA are adsorbed on the surface of fine particles. Meanwhile, some fine particles are attached to the surface of the micro-bubbles. The adsorption and attachment enhance the surface strength of micro-bubbles, such that they will not easily burst under pressure. These micro-bubbles fill in and reinforce the mesh structure and the voids in coarse aggregates.

With a smaller density, the micro-bubbles will move upward by buoyancy in cement slurry, carrying fine particles along the way. If the mesh structure formed by SA is incomplete and defective, the micro-bubbles, together with fine particles, will come out of slurry surface through the defects in the system. After fine particles leave the system, the coarse aggregates will accumulate and sediment, and eventually result in delamination [24, 25].

Moreover, the top and bottom of cement slurry will become inhomogeneous, as lots of cement particles, fly ash, fine mud aggregates and water are clustered on the surface. This will slow down the formation of the floc structure of cement hydrates. The water evaporation determines the subsidence of hardened slurry block in mold (Figure 4a), which exhibits as the condensation of Group 3.

Groups 3 and 4 had the same AEA dosage, but the Group 4 had a slightly higher SA dosage. When the SA dosage is insufficient, the mesh structure has good integrity and coverage. The micro-bubbles, which are produced by AEA adsorbing fine particles, are bound to the mesh structure. Then, the micro-bubbles will not move upward, and the coarse aggregates will not sediment. In this way, the cement slurry becomes more homogenous and flowable [26]. To meet the requirements of long-distance piping, the optimal dosages of SA and AEA were determined as 0.045% and 0.009%, respectively.

5.3 Verification of synergy mechanism

According to the XRD images on hardened blocks of Groups 3 and 4 after 28d-long curing, the blocks of the two groups had basically the same kinds of cement hydrates: AFt phase and C-S-H gel. The needle-like AFt interspersed in C-S-H gel, providing strength for the hardened blocks [27, 28]. The cement hydration reactions include: (2)

When fly ash is added into the slurry, $Ca(OH)_2$ reacts with SiO_2 and Al_2O_3, producing AFt phase and C-S-H gel in the hardened blocks.

Then, SEM experiments were carried out hardened blocks of Groups 3 and 4 after 28d-long curing. As shown in Figure 7a, the cement hydrates on the top of the hardened block of Group 3 were denser than those on the bottom of that block. The skeleton structure is formed by the overlapping of AFt phase, which is bonded by C-S-H gel into a mesh structure that strengthens the hardened blocks [29, 30]. Compared with the top surface, the bottom of the hardened block of Group 3 had many interspaces of hydrates that are loosely overlapped. The inhomogeneity of the hydrates inside this block is attributable to the fact that the micro-bubbles produced by AEA drive fine particles to the top surface, making the hydrate content greater on the top than on the bottom.

As shown in Figure 7b, the top and bottom of the hardened block of Group 4 were homogenous and similarly dense in terms of cement hydrates. This is because the block of Group 4 has a greater dosage of SA than the block

$$\begin{cases} 2(3CaO\cdot SiO_2)+6H_2O=3CaO\cdot 2SiO_2\cdot 3H_2O+3Ca(OH)_2 \\ 2(2CaO\cdot SiO_2)+4H_2O\rightarrow 3CaO\cdot 2SiO_2\cdot 3H_2O+Ca(OH)_2 \\ 3CaO\cdot Al_2O_3+6H_2O\rightarrow 3CaO\cdot Al_2O_3\cdot 6H_2O \\ 4CaO\cdot Al_2O_3\cdot Fe_2O_3+7H_2O\rightarrow 3CaO\cdot Al_2O_3\cdot 6H_2O+CaO\cdot Fe_2O_3\cdot H_2O \\ 3CaO\cdot Al_2O_3\cdot 6H_2O+3(CaSO_4\cdot 2H_2O)+19H_2O\rightarrow 3CaO\cdot Al_2O_3\cdot 3CaSO_4\cdot 31H_2O \end{cases} \tag{2}$$

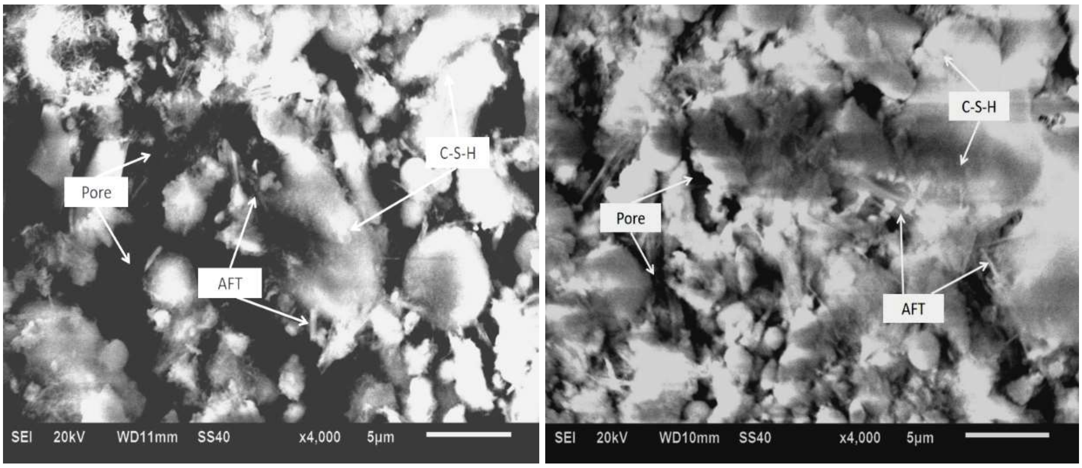

Top Bottom

(a) SEM images of the hardened block of Group 3

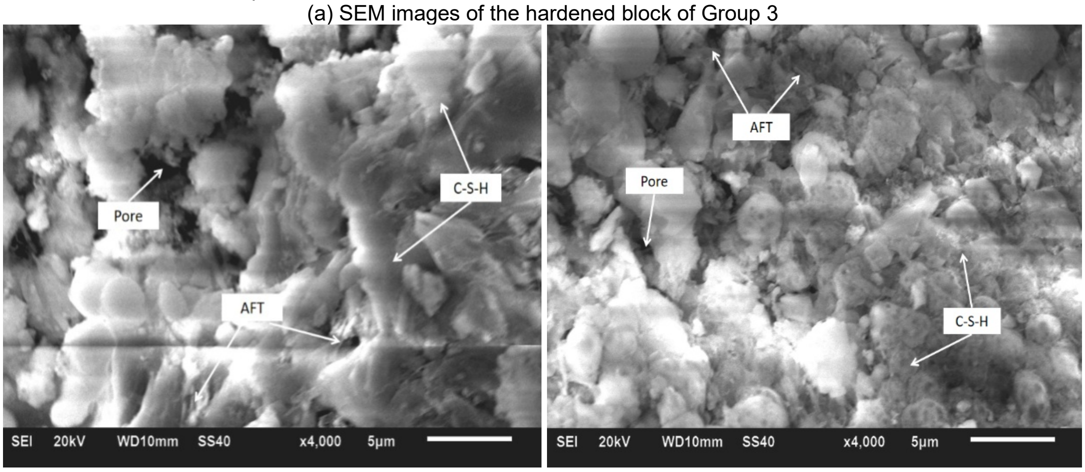

Top Bottom

(b) SEM images of the hardened block of Group 4

Fig.7 - SEM images of hardened blocks

of Group 3. The high SA dosage binds the micro-bubbles with fine particles into a complete mesh structure. Hence, the block of Group 4 has a relatively good homogeneity, without internal condensation.

Furthermore, the hydrates in the blocks of Groups 3 and 4 differed in the degree of crystallization. The crystallization degree of hydrates in the block of Group 4 was higher than that of the block of Group 3. This also proves that the SA and AEA dosages are more suitable in Group 4.

6. Conclusions

(1) The rheological patterns of the four groups of cement slurries were homogeneous Bingham patterns at 0, 30, 60, and 90min, respectively. The rheological patterns of Groups 2 and 3 both changed to pseudoplastics flow pattern at 120min. Groups 2 and 3 cement slurries maintained good flowability at 120min. However, the two slurries had intense coal gangue sedimentation, pushing up the risk of pipe blockage in long-distance transport. The cement slurry of Group 4 featured good flowability and no sedimentation, meeting the requirements on long-distance piping.

(2) The SA DF can homogenize the cement slurry, while the AEA ST can increase the flowability of the slurry. If the two agents are combined in reasonable dosages, the cement slurry will obtain long-term rheological stability in long-distance piping. The reasonable dosages were determined as 0.045% for the SA and 0.009% for the AEA.

(3) SEM and XRD images confirm the inhomogeneity of the hardened block of Group 3, as evidenced by the subsidence on the top surface. Meanwhile, the hardened block of Group 4 achieved homogeneity, indicating that the cement slurry in this group is suitable for long-distance pipeline transportation.

Acknowledgments

This study is sponsored by National Key R&D Plan of China (2017YFC0603002), Basic Scientific Research Expenses Project of Provincial Colleges and Universities in Heilongjiang Province (Hkdcx201801) and Joint Guiding Project of Natural Science Fund of Heilongjiang Province (LH2019E119)

REFERENCES

[1] B.G. Yang, J. Yang, Y. Yu, D. Li, B. Jiang, and K. Cheng, Study on proportioning test of a new cementing filling material and hydration mechanism. Journal of Mining Science and Technology, 2017, **2**(5), 475-488.

[2] J. Ye, J.X. Xia, and M. Beata, Study on the resistance loss of hydraulic transport for coarse particles in horizontal pipeline. Metal Mine, 2011, **7**, 12-18.

[3] D.Q. Deng, Y.J. Zhu, F.Z. Wang, L. Wang, and W.J. Yu, Transportation numerical simulation of cement slurry in long distance pipeline. Journal of Anhui University (Natural Science Edition), 2012, **6**, 36-43.

[4] W.B. Xu, B.G. Yang, S.L. Yang, and P. Dang, Experimental study on correlativity between rheological parameters and grain grading of coal gauge backfill slurry. Journal of Central South University(Science and Technology), 2016, **47**, 1282-1289.

[5] J. Yang, J.L. Wu, and J.Y. Jin, Study on the suspended properties of gangue particles with high concentration of gangue and fly ash. Journal of Mining Science and Technology, 2019, **4**, 127-132.

[6] D. Deb, T. Sreenivas, G.K. Dey, and S. Panchal, Paste backfill technology: essential characteristics and assessment of its application for mill rejects of uranium ores. Transactions of the Indian Institute of Metals, 2017, **70**(2), 487-495.

[7] R. Anubhav, S.N. Singh, and V. Seshadri, Computational methodology for determination of head loss in both laminar and turbulent regimes for the flow of high concentration coal ash slurries through pipeline. Particulate Science and Technology. 2016, **34**(3), 289-300.

[8] J.K. Lee, J.Q. Shang, S. Jeong, Thermal conductivity of compacted fill with mine tailings and recycled tire particles. Soils and Foundations, 2015, **55**(6), 1454-1465.

[9] M. Brunel, W. Wichitwong, S. Coetmellec, A. Masselot, D. Lebrun, G. Gréhan, and G. Edouard, Numerical models for exact description of in-situ digital in-line holography experiments with irregularly-shaped arbitrarily-located particles. *Applied Sciences*, 2015, ***5***(2), 62-76.

[10] J. Wu, L. Li, X. Du, and X. Liu, Numerical study on the asphalt concrete structure for blast and impact load using the Karagozian and case concrete model. Applied Sciences, 2017, **7**(2), 202.

[11] M.G. Qian, J.L. Xu, and X.X. Miao, Green technique in coal mining. Journal of China University of Mining & Technology. 2003, **32**(4), 343-348.

[12] X.X. Miao, and M.G. Qian, (2009). Research on green mining of coal resources in China: current status and future prospects. Journal of Mining & Safety Engineering, 2009, **26**, 1-14.

[13] H. Hu, H.H. Sun, and Y.C. Huang, Analysis of rheological characteristics and multi-factor influence of cement slurry with similar paste. Nonferrous Metals, 2003, **3**, 4-7.

[14] W.S. Aaron, M.J. Hamlin, and P.S. Surendra, A generalized approach for the determination of yield stress by slump and flow. Cement and Concrete Research, 2004, **34**(3), 363-371.

[15] X. He, M. Ma, Y. Su, M. Lan, Z. Zheng, T. Wang, B. Strnadel, and S. Zeng, The effect of ultrahigh volume ultrafine blast furnace slag on the properties of cement pastes. Construction and Building Materials, 2018, **189**, 438-447.

[16] T. Li, T. Qin, Y.B. Zhou, Y. Bi, and X. Wang, Chemical properties of bingham materials in backfilling. Chemical Engineering Transactions, 2018, **71**, 1057-1062.

[17] Z. Qiu, T. Cao, Y. Li, J. Wang, and Y. Chen, Rheological behavior and modeling of a crushed sandstone mudstone particle mixture. Processes, 2018, **6**(10), 192.

[18] T.S. Khan, Y. Dai, M.S. Alshehhi, and L. Khezzar, Experimental flow characterization of sand particles for pneumatic transport in horizontal circular pipes. Power Technol, 2016, **292**, 158-168.

[19] A. Ghirian, and M. Fall, Coupled behavior of cemented paste backfill at early ages. Geotechnical and Geological Engineering, **33**(5), 1141-1166.

[20] J. Guo, Study on the global rheology and local flow mechanism of concentrated suspensions. Shanghai Jiao Tong University, Shanghai, China, 2011.

[21] D. Wu, B.G. Yang, and Y.C. Liu, Transportability and pressure drop of fresh cemented coal gangue-fly ash backfill slurry in pipe loop, Powder Technology, 2015, **284**, 218-224.

[22] F. Haq, H. Yu, L. Wang, L. Teng, M. Haroon, R.U. Khan, S. Mehmood, B-Ul-Amina, R.S. Ullah, A. Khan, and A. Nazir, Advances in chemical modifications of starches and their applications. Carbohydrate Research, 2019, **476**, 12-35.

[23] R.J. Gao, H. Wu, L. Wang, and Y. Yao, Effect and mechanism of machine-made sand stone powder on rheological properties of cement-based materials. Bulletin of the Chinese Ceramic Society, 2019, **4**, 1080-1085.

[24] S.Z. Wang, Suspension, stability and homogeneity of slurry in long distance pipeline transportation. Hydraulic Coal Mining & Pipeline Transportation, 1994, **2**, 30-33.

[25] L. Cui, and M. Fall, An evolutive elasto-plastic model for cemented paste backfill. Computers and Geotechnics, **71**, 19-29.

[26] L.T. Zou, Experimental study on rheological properties and drag reduction mechanism of three-phase flow. Journal of Sediment Research, 1996, **2**, 22-29.

[27] D.P. Bentz, C.F. Ferraris, M.A. Galler, A.S. Hansen, and J.M. Guynn, Influence of particle size distributions on yield stress and viscosity of cement–fly ash pastes. Cement and Concrete Research, 2012, **42**(2), 404-409.

[28] B. Wang, T. Wu, H.J. Dai, and G. Bai, Numerical study on the seismic performance of a steel concrete hybrid supporting structure in thermal power plants. Applied Sciences, **8**(2), 294.

[29] Y. Dong, X.B. Yang, and Q. Gao, Research on effect of pore characteristics on performance of aerated backfilling concrete based on imaging method. Material Guide, 2018, **9**, 3128-3134.

[30] B.G. Yang, Y.T. Liang, and Y.K. Wang, Admixture ratio of high concentration cementation backfilling materials in coal mine. EJGE. 2015, **20**, 10091-10101.

****